Chaos in time-dependent variational approximations to quantum dynamics

Fred Cooper,[1] John Dawson,[2] Salman Habib,[1] and Robert D. Ryne[3]
[1]*T-8, Theoretical Division, MS B285, Los Alamos National Laboratory, Los Alamos, New Mexico 87545*
[2]*Department of Physics, University of New Hampshire, Durham, New Hampshire 03824*
[3]*LANSCE-1, LANSCE Division, MS H817, Los Alamos National Laboratory, Los Alamos, New Mexico 87545*
(Received 29 October 1996; revised manuscript received 1 October 1997)

Dynamical chaos has recently been shown to exist in the Gaussian approximation in quantum mechanics and in the self-consistent mean field approach to studying the dynamics of quantum fields. In this study, we first note that any variational approximation to the dynamics of a quantum system based on the Dirac action principle leads to a classical Hamiltonian dynamics for the variational parameters. Since this Hamiltonian is generically nonlinear and nonintegrable, the dynamics thus generated can be chaotic, in distinction to the exact quantum evolution. We then restrict our attention to a system of two biquadratically coupled quantum oscillators and study two variational schemes, the leading order large-N (four canonical variables) and Hartree (six canonical variables) approximations. The chaos seen in the approximate dynamics is an artifact of the approximations: this is demonstrated by the fact that its onset occurs on the same characteristic time scale as the breakdown of the approximations when compared to numerical solutions of the time-dependent Schrödinger equation. [S1063-651X(98)04301-3]

PACS number(s): 05.45.+b, 03.65.Sq, 02.30.Wd

I. INTRODUCTION

There are many situations in quantum mechanics and field theory where one hopes that one dynamical degree of freedom can be considered ''classical'' or ''semiclassical.'' In the dynamics of the early Universe, one usually imagines that gravitational energy can be transferred to particle production, with the gravitational field being treated semiclassically; i.e., the quantum matter fields evolve in a background ''classical'' gravitational field, the dynamics of which is in turn determined from the expectation value of the energy momentum tensor of the quantum field. Similarly in pair production from strong electric fields, one attempts to describe the background electric field ''classically'' and solve for the dynamics of the quantum degrees of freedom in this background field. The time dependence of the electric field is governed by a Maxwell equation in which the right hand side is the average value of the current of the produced pairs. In this sort of approximation of a quantum system coupled with a semiclassical degree of freedom such as a coherent electric or gravitational field, the *approximate* dynamics of the quantum system can become chaotic. This was first described by us, and termed ''semiquantum chaos'' [1,2]. A closely related result having the same cause is ''semiquantal chaos'' [3], which occurs in the time-dependent Gaussian approximation for the dynamics of quantum systems. The existence of chaos in the general case of dynamical variational approaches was noted by Caurier *et al.* [4] who also argued that the onset of chaos signaled the breakdown of the approximation scheme.

What happens in these dynamical approximations is that the time evolution of the parameters governing the shape of the quantum mechanical wave function (or functional) becomes sensitive to the initial conditions. We will first present an argument as to why this behavior can occur in *any* variational approximation to the quantum dynamics (e.g., time-dependent Hartree approximation). Next we will focus on exactly the same model system treated in Refs. [1,2], namely, a system of two coupled oscillators described by the Lagrangian

$$L = \tfrac{1}{2}\dot{A}^2 + \tfrac{1}{2}\dot{x}^2 - \tfrac{1}{2}(m^2 + e^2A^2)x^2. \tag{1.1}$$

This system of two nonlinearly coupled oscillators arose from studying the problem of pair production of charged pions in a strong external electric field [5] (quantum fluctuations of the electric field were ignored). In momentum space, the individual modes of the pion field displayed chaotic behavior. The two-oscillator problem results from ignoring all but the $k=0$ mode for the quantum field. In the Lagrangian (1.1), the A oscillator represents the time-dependent electromagnetic field and the x oscillator, the $k=0$ mode of the charged pion field.

Treating the electromagnetic (A) field classically is the standard first term in a large-N expansion [6] and is related to the classic problem treated first by Schwinger [7] on pair production from external fields. Because such semiclassical methods are often used in initial value problems in quantum field theory, we hope to understand the origin of the chaos by considering a simple quantum mechanical model. To this must be added the important point that while accurate numerical solutions to the quantum mechanical problem are available to test the validity of approximations, such a luxury is not available in field theory.

The semiclassical calculation is equivalent to a Gaussian variational approximation to the field theory (see Ref. [8] for more details and an explanation of dissipation and decoherence in this approximation). As shown later, all variational approximations to quantum dynamics lead to classical Hamiltonian dynamics for the variational parameters (the Gaussian approximation is a special case), a result due originally to Kan [9]. Since the dynamics is generically nonlinear, it can be chaotic.

We will consider two variational approximations that make two different assumptions about the fluctuations of the A oscillator. The first approximation (leading order large N) is the assumption that we can ignore *all* quantum fluctuations of the A oscillator (the quantum mechanical version of the electromagnetic field). This is equivalent to assuming

$$\langle A^2 x\rangle = \langle A\rangle^2 \langle x\rangle. \tag{1.2}$$

The Hartree approximation includes only Gaussian fluctuations of *both* quantum oscillators. This implies a factorization of the expectation values as

$$\langle A^2 x\rangle = \langle A^2\rangle \langle x\rangle. \tag{1.3}$$

Both of these approximations include only Gaussian fluctuations and are dynamically equivalent to the corresponding classical Liouville equation when only Gaussian fluctuations are allowed, with a particular initial condition implementing the uncertainty relation. Consequently, the same chaos discussed above will also be found in the classical theory. This aspect of the Gaussian approximation we will discuss elsewhere [10].

Our numerical results show that in the Hartree approximation, the onset of chaos, as a function of parameters of the Hamiltonian, is marginally delayed as compared to the large-N (semiclassical) approximation. We find that both approximations diverge from the exact numerical simulation of the Schrödinger equation at approximately the same time. After that time, the Hartree approximation qualitatively tracks the general features of the exact simulation better than the large-N approximation. By direct comparison with the exact numerical solution we also find that chaos in the variational approximations occurs roughly on the same time scale as when these approximations diverge from the exact numerical solution. As is known on general grounds [11], expectation values of the full quantum system (which are the variational parameters of the classical Hamiltonian dynamics) are insensitive to initial conditions: our results are completely consistent with this fact. Our interpretation of the above results is in accord with that of Refs. [4,12] who have argued that the chaos seen in the approximate dynamics is not a fundamental feature of the full quantum dynamics but simply reflects a breakdown of the approximation scheme. It was further argued in Ref. [12] that the approximations are unreliable when either the classical equations are already chaotic or when the approximate dynamics is chaotic. To test the second part of this statement we explored nonchaotic parameter regimes for the approximate dynamics (but not too far from the onset of chaos) and found essentially no improvement in the agreement between the exact quantum and approximate calculations. Thus the existence of chaos is insufficient to assess the accuracy of the approximations: apparently the breakdown time (in terms of natural time scales) is the same whether chaos is present or not.

It is strong nonlinearity rather than just chaotic dynamics that leads to the breakdown of the approximations. This is hardly surprising: the Gaussian approximations are equivalent to truncating a cumulant expansion at second order. If the exact dynamics is strongly nonlinear, higher order cumulants are generated and a second order truncation quickly becomes invalid. For chaotic systems, Ref. [12] provides a simple analytic argument, but the statement is true more generally.

These results might seem to put very strong constraints on dynamical mean field approximations in quantum field theory, especially at strong coupling. However, the field theoretic analog to the above problem has a very large (formally infinite) number of degrees of freedom. For example, in the field theoretic case, Eq. (1.1) is a radical truncation of the full Lagrangian

$$L = |(\partial_\mu - ieA_\mu)\phi|^2 - \frac{1}{4}(\partial_\mu A_\nu - \partial_\nu A_\mu)^2 - m^2\phi^\dagger\phi. \tag{1.4}$$

In the leading order large-N approximation, A is still treated classically but it is now coupled to a very large number of fluctuating degrees of freedom. Before definitive statements regarding the accuracy of mean field approximations can be made, two issues have to be clarified. The first has to do with the fact that even though the individual trajectories of the Fourier modes ϕ_k may be chaotic and far from the exact solution, what really matters is the summed contribution (i.e., the statistics of the distribution of trajectories) and this may have a much more benign character. The second point is related to the onset of chaos as the number of degrees of freedom is varied. The importance of this question was noted by Ford [13] but it has not been studied in any detail in the literature. Thus, it is still an open question whether chaos in the mean field approximation in field theory is as serious an obstruction as suggested by the study of lower dimensional systems.

The rest of the paper is set out as follows. First (Sec. II) we prove the general result that all variational approximations lead to a Hamiltonian dynamics for the variational parameters. Then, in Sec. III we explicitly discuss the Hamiltonian dynamics for the two oscillator problem, both in the large-N and Hartree approximations. In Sec. IV we briefly describe our numerical approach to the exact solution of the two coupled oscillator problem. We then compare numerical simulations of the two variational approximations with the exact solution of the Schrödinger equation. Finally, in Sec. V, we state our conclusions and discuss the implications of our results.

II. THE TIME-DEPENDENT VARIATIONAL PRINCIPLE

The Schrödinger equation can be reduced to a system of ordinary differential equations for some variational parameters by constraining the wave function to be of a particular form. The fact that any variational calculation of the wave function will lead to a Hamiltonian dynamics for the variational parameters was first noted by Kan [9]. Here we provide an alternative, compact derivation.

The starting point for a variational calculation is Dirac's action principle [14], which can also be used to derive the Schrödinger equation as shown below. We begin by defining the action

$$S = \int_{t_1}^{t_2} dt \left\langle \Psi \left| i\frac{\partial}{\partial t} - H \right| \Psi \right\rangle / \langle \Psi | \Psi \rangle. \tag{2.1}$$

The time-dependent Schrödinger equation

$$\left(i\frac{\partial}{\partial t} - H \right) |\Psi\rangle = 0 \tag{2.2}$$

then follows from the variational principle $\delta S = 0$ along with the boundary conditions $\delta|\Psi(t_1)\rangle = 0;\ \delta|\Psi(t_2)\rangle = 0$.

Minimizing the action (2.1) on a restricted variational basis for the wave function

$$\Psi \rightarrow \Psi_v(y_i(t)), \quad \int dt \Psi_v^* \Psi_v = 1 \tag{2.3}$$

leads to an effective action functional defined on the variational parameters $y_i(t)$:

$$\Gamma[y_i(t)] = \int dt \left\langle \Psi_v \left| i\frac{\partial}{\partial t} - H \right| \Psi_v \right\rangle, \tag{2.4}$$

where the wave function is usually given in the coordinate representation. Extremization of the effective action via $\delta\Gamma[y_i] = 0$ yields the dynamical equations obeyed by the variational parameters.

In order to show that any variational solution leads to a symplectic Hamiltonian dynamics for the variational parameters (the case of Gaussians was considered in Ref. [15]), we consider general trial wave functions that are completely determined by n time-dependent functions of the form $y_i(t)$, $i = 1, \ldots, n$, and written formally as

$$\Psi(x,t) = \Psi(x; y_i(t)). \tag{2.5}$$

Here we choose for simplicity a one-dimensional Schrödinger equation with arbitrary potential. Note that the entire time dependence of the wave functions is contained in the variational functions $y_i(t)$. The Dirac form of the action is then given by

$$\begin{aligned} \Gamma[y] &= \int dt \int_{-\infty}^{+\infty} dx\, \Psi^*(x; y(t)) \left\{ i\frac{\partial}{\partial t} - H \right\} \Psi(x; y(t)) \\ &= \int dt\, L(y, \dot{y}), \end{aligned} \tag{2.6}$$

with H given by

$$H = -\frac{1}{2}\frac{d^2}{dx^2} + V(x). \tag{2.7}$$

Given the above parametric form of the wave function, $L(y,\dot{y})$ is *always* given by a function of the form

$$L(y,\dot{y}) = \sum_{i=1}^{n} \pi_i(y)\dot{y}_i - h(y), \tag{2.8}$$

where

$$\begin{aligned} \pi_i(y) = \int_{-\infty}^{+\infty} dx \frac{i}{2} \Big\{ & \Psi^*(x;y) \frac{\partial}{\partial y_i} \Psi(x;y) \\ & - \Psi(x;y) \frac{\partial}{\partial y_i} \Psi^*(x;y) \Big\} \end{aligned} \tag{2.9}$$

and

$$h(y) = \int_{-\infty}^{+\infty} dx\, \Psi^*(x;y) H \Psi(x;y). \tag{2.10}$$

Minimization of the action, Eq. (2.6), leads to Lagrange's equations:

$$\frac{d}{dt}\frac{\partial L}{\partial \dot{y}_i} - \frac{\partial L}{\partial y_i} = 0 \quad \text{for} \quad i = 1,n. \tag{2.11}$$

The equations of motion for y_i can be found easily using the specific Lagrangian defined in Eq. (2.8),

$$\sum_{j=1}^{n} M_{ij}(y)\dot{y}_j = \frac{\partial h(y)}{\partial y_i}, \tag{2.12}$$

where $M_{ij}(y)$ is an antisymmetric matrix given by

$$M_{ij}(y) = \frac{\partial \pi_i}{\partial y_j} - \frac{\partial \pi_j}{\partial y_i} = -M_{ji}(y). \tag{2.13}$$

If the inverse of M_{ij} exists, the equations of motion can be put in a symplectic form:

$$\dot{y}_i = \sum_{j=1}^{N} M_{ij}^{-1}(y) \frac{\partial h(y)}{\partial y_j}. \tag{2.14}$$

Since M_{ij}^{-1} is also antisymmetric, $h(y)$ is a conserved quantity:

$$\frac{dh(y)}{dt} = \sum_i \frac{\partial h}{\partial y_i}\dot{y}_i = \sum_{ij} \frac{\partial h}{\partial y_i} M_{ij}^{-1} \frac{\partial h}{\partial y_j} = 0. \tag{2.15}$$

Following Das [16], we now introduce Poisson brackets by

$$\{A,B\} = \sum_{ij} \frac{\partial A(y)}{\partial y_i} M_{ij}^{-1} \frac{\partial B(y)}{\partial y_j}. \tag{2.16}$$

So, for example,

$$\{y_i, y_j\} = M_{ij}^{-1}. \tag{2.17}$$

The equations of motion can now be written in terms of these Poisson brackets:

$$\dot{y}_i = \{y_i, h(y)\} = \sum_j M_{ij}^{-1} \frac{\partial h}{\partial y_j} = \sum_j \{y_i, y_j\} \frac{\partial h}{\partial y_j}. \tag{2.18}$$

The antisymmetry of the Poisson brackets is explicit in their definition (2.17). However, they must also obey Jacobi's identity:

$$\{y_i, \{y_j, y_k\}\} + \{y_j, \{y_k, y_i\}\} + \{y_k, \{y_i, y_j\}\} = 0, \tag{2.19}$$

which is satisfied if M_{ij} obeys Bianchi's identity:

$$\frac{\partial M_{ij}}{\partial y_k} + \frac{\partial M_{ki}}{\partial y_j} + \frac{\partial M_{jk}}{\partial y_i} = 0. \tag{2.20}$$

But Bianchi's identity is always satisfied for M_{ij} of the form

$$M_{ij}=\partial_i\pi_j-\partial_j\pi_i. \tag{2.21}$$

Thus our definition of the Poisson brackets satisfies Jacobi's identity, and the set of classical equations of motion (2.18) are symplectic.

III. HARTREE APPROXIMATION AND THE LARGE-N LIMIT

We have shown that a time-dependent variational approximation always leads to a Hamiltonian dynamical system for the variational parameters. Since such a system is generically nonlinear, there is a strong likelihood of chaos in the phase space of these Hamiltonian parameters. In this section we derive two different approximations for the coupled oscillator problem. The first keeps Gaussian correlations (Hartree approximation) for both oscillators, while the second (large-N approximation) ignores fluctuations in the A oscillator. The second approximation has been derived previously from a path integral approach [2] by making N copies of the x oscillator and then taking the large N limit.

The model Hamiltonian that generalizes the two-oscillator problem to an $N+1$ oscillator system is

$$H=\frac{1}{2}p_A^2+\sum_{i=1}^{N}\frac{1}{2}p_i^2+\frac{1}{2}(m^2+e^2A^2)\sum_{i=1}^{N}x_i^2, \tag{3.1}$$

where we have introduced an $N+1$ component oscillator x_μ; $\mu=0,1,\ldots,N$ with $x_0=A$ and the other N oscillators labeled by the roman indices $i=1,2,\ldots,N$. We show below that at large N, a Gaussian ansatz for the wave function reproduces the exact large-N limit of the quantum mechanical system. At $N=1$, the Gaussian approximation reduces to the well known Hartree approximation.

The operator equations of motion following from the Hamiltonian (3.1) are

$$\ddot{x}_i+(m^2+e^2A^2)x_i=0, \tag{3.2}$$

$$\ddot{A}+e^2\sum_i x_i^2A=0. \tag{3.3}$$

Taking expectation values of these two equations we obtain

$$\langle\ddot{x}_i\rangle+m^2\langle x_i\rangle+e^2\langle A^2x_i\rangle=0, \tag{3.4}$$

$$\langle\ddot{A}\rangle+e^2\langle x^2A\rangle=0. \tag{3.5}$$

It was shown in Ref. [2] that in the large-N limit, fluctuations of the A oscillator are suppressed by $1/N$ and the exact equations (3.4) and (3.5) are approximated by

$$\langle\ddot{x}_i\rangle+m^2\langle x_i\rangle+e^2\langle A\rangle^2\langle x_i\rangle=0, \tag{3.6}$$

$$\langle\ddot{A}\rangle+e^2\langle x^2\rangle\langle A\rangle=0. \tag{3.7}$$

The semiclassical field $\langle A\rangle$ now has a time-dependent mass given by the quantum expectation value $\langle x^2\rangle$. The quantum oscillator x_i has a mass with time dependence controlled by $\langle A\rangle$. (This system was discussed in detail in Refs. [1,2].) It is also perfectly clear that the large-N limit is equivalent to treating the A oscillator classically (i.e., ignoring the quantum fluctuations about the mean value of A).

The equations governing $\langle A\rangle$ and $\langle x^2\rangle=G$ when $\langle x\rangle=0$ were shown to be derivable [1] from the effective classical Hamiltonian:

$$H_{\rm eff}=\frac{1}{2}p_A^2+2\hbar\Pi_G^2G+\frac{\hbar}{8G}+\frac{\hbar}{2}(m^2+e^2A^2)G. \tag{3.8}$$

We will show below that using a Gaussian trial wave function in Dirac's variational principle and taking the large-N limit will lead to the same effective Hamiltonian (3.8) for the evolution of the expectation values. However, if instead of taking the large-N limit, we set $N=1$, and a trial wave function that is a product of Gaussians in A and x, then the equations for the expectation values become

$$\langle\ddot{x}_i\rangle+m^2\langle x_i\rangle+e^2\langle A^2\rangle\langle x_i\rangle=0, \tag{3.9}$$

$$\langle\ddot{A}\rangle+e^2\langle x^2\rangle\langle A\rangle=0. \tag{3.10}$$

Here $\langle A^2\rangle=\langle A\rangle^2+D$, and D is the Gaussian quantum fluctuation of the A oscillator (which also is the width of the A wave function). In this case we will also get an effective Hamiltonian description of the dynamics, but with two more parameters, D and Π_D. We will compare these two approximate Hamiltonian dynamics with the numerical simulation of the exact dynamics.

Our choice for the trial wave function is

$$\Psi_v(x_\mu)=N\exp\left[-\frac{1}{\hbar}[x-q(t)]_\mu[x-q(t)]_\nu\left(\frac{G^{-1}}{4}-i\Pi\right)_{\mu\nu}+\frac{i}{\hbar}p_\mu(t)[x-q(t)]_\mu\right], \tag{3.11}$$

where the normalization constant is given by

$$N=\exp\left[-\frac{1}{4}\mathrm{Tr}\ln(2\pi\hbar G)\right].$$

The variational parameters are related to various expectation values taken with respect to the variational wave function Ψ_v:

$$q_i(t)=\langle\Psi_v|x_i|\Psi_v\rangle,$$

$$p_i(t)=-\left\langle\Psi_v\left|i\hbar\frac{\partial}{\partial x_i}\right|\Psi_v\right\rangle, \tag{3.12}$$

$$G_{ij}(t)+q_i(t)q_j(t)=\langle\Psi_v|x_ix_j|\Psi_v\rangle,$$

$$2q_i(t)p_j(t)+4\Pi_{ik}(t)G_{kj}(t)=\langle\Psi_v|x_ip_j+p_jx_i|\Psi_v\rangle.$$

The equations for these expectation values are obtained by varying the effective action, or equivalently from Hamilton's equations using the effective Hamiltonian.

The effective action for the variational parameters p,q,G,Π is

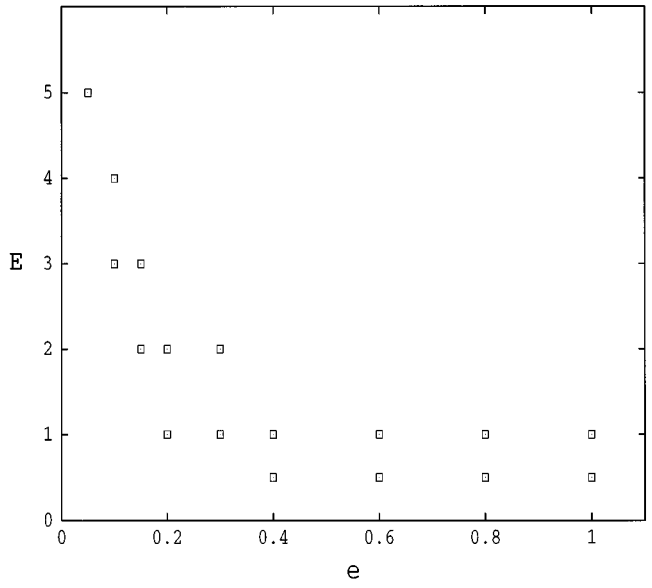

FIG. 1. Domain of integrability for the large-N approximation in energy and coupling constant space. The phase space was sampled with ten initial conditions at each (e,E) point and trajectories asymptoting to positive Lyapunov exponents were searched for. At fixed e, the region above any point denoted by the top square in the figure corresponds to chaotic dynamics, i.e., in the set of trajectories sampled there was at least one with asymptotically positive Lyapunov exponent. The region below the bottom square corresponds to integrable dynamics.

$$\Gamma=\int dt\left\{\sum_{i=1}^{N} p_i\dot{q}_i+p_A\dot{A}-\hbar\,\mathrm{Tr}[\dot{\Pi}G]-H_{\mathrm{eff}}\right\}, \tag{3.13}$$

where $\mathrm{Tr}[AB]=A_{\mu\nu}B_{\nu\mu}$ and the effective Hamiltonian,

$$\begin{aligned}H_{\mathrm{eff}}&=\langle\Psi_v|H|\Psi_v\rangle\\&=\sum_{i=1}^{N}\frac{p_i^2}{2}+\frac{p_A^2}{2}+\hbar\,\mathrm{Tr}\left[\frac{1}{8}G^{-1}\right]+2\hbar\,\mathrm{Tr}[\Pi G\Pi]\\&\quad+\left[\frac{m^2}{2}+\frac{e^2}{2}(A^2+G_{00})\right]\sum_{i=1}^{N}(q_i^2+G_{ii}).\end{aligned} \tag{3.14}$$

This last equation gives the effective Hamiltonian for the dynamics of the $N+1$ oscillators in the Hartree approximation. For simplicity (as was done in Ref. [1]), we now specialize to the case $q(t)=p(t)=0$. In this case G and Π are diagonal (in general, they are also diagonal to leading order in the $1/N$ expansion). Since we have N replicas of the x oscillator, the diagonal condition simply means that $G_{ij}(t)=G(t)\delta_{ij}$. Inserting this condition in Eq. (3.14) we find

$$\begin{aligned}H_{\mathrm{eff}}^{(0)}&=\frac{1}{2}p_A^2+2\hbar(N\Pi_G^2G+\Pi_D^2D)+\frac{\hbar}{8}\left(\frac{N}{G}+\frac{1}{D}\right)\\&\quad+\frac{\hbar N}{2}[m^2+e^2(A^2+\hbar D)]G.\end{aligned} \tag{3.15}$$

Setting $N=1$ in Eq. (3.15), we find the effective Hamiltonian that controls the Hartree approximation:

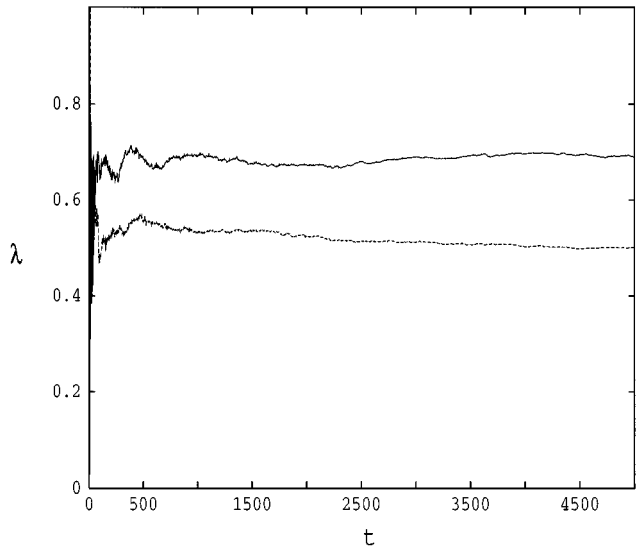

FIG. 2. A typical computation of the maximal Lyapunov exponents for the large N (upper curve) and Hartree (lower curve) approximations. Parameter values for this run were $e=1$ and $E=5$.

$$\begin{aligned}H_H^{(0)}&=\frac{1}{2}p_A^2+2\hbar(\Pi_G^2G+\Pi_D^2D)+\frac{\hbar}{8}\left(\frac{1}{G}+\frac{1}{D}\right)\\&\quad+\frac{\hbar}{2}[m^2+e^2(A^2+\hbar D)]G,\end{aligned} \tag{3.16}$$

where $G=G_{11}$ and $D=G_{00}$.

Next we take the large-N limit of Eq. (3.15) using the same scaling argument as in determing the large-N limit of the path integral formulation [2]: we let $A\to\sqrt{N}\widetilde{A}$ and $p_A\to\widetilde{p}_A$ (leaving invariant $eA=\widetilde{e}\widetilde{A}$). Dividing the effective Hamiltonian by N and keeping the leading term, we find that the large-N Gaussian effective Hamiltonian is exactly the same as the effective Hamiltonian found from the leading order large N action [2]. The rescaled effective Hamiltonian reads

$$\begin{aligned}\widetilde{H}_{\mathrm{eff}}^{(0)}&=H_{\mathrm{eff}}^{(0)}/N\\&=\frac{1}{2}p_A^2+2\hbar\Pi_G^2G+\frac{\hbar}{8G}+\frac{\hbar}{2}(m^2+e^2A^2)G,\end{aligned} \tag{3.17}$$

which is in complete agreement with Eq. (3.8). (Tildes denoting the rescaled variables have been suppressed above.) At $N=1$, the Hartree approximation has two more variational parameters D and Π_D compared to the large-N approximation. These are related to the real and imaginary parts of the width of the wave function for the A oscillator and are obviously not incorporated in the large-N approximation. Because of the extra degrees of freedom incorporated in it, one might anticipate Hartree to be the better of the two approximations.

In the Hartree approximation, the Hamilton's equations for the expectation values are

$$\dot{A}=p_A,\quad \dot{p}_A=-e^2\hbar AG, \tag{3.18}$$

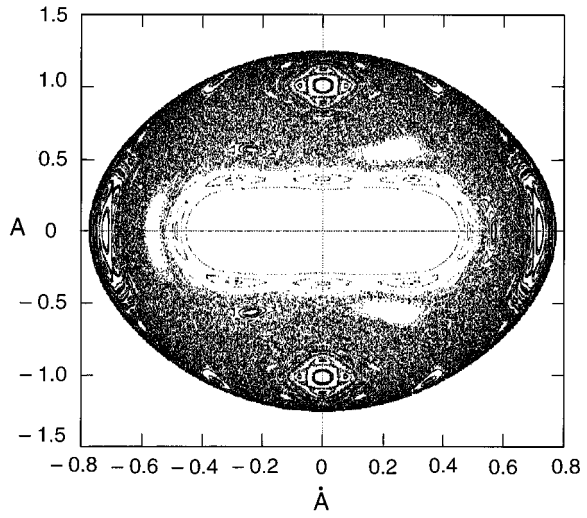

FIG. 3. A Poincaré section in the A, $\dot{A}$ plane for $e=1$ and $E=0.8$ for the large-N approximation. The phase space was sampled by 256 different trajectories.

$$\dot{G}=4\hbar\Pi_G G, \quad \dot{D}=4\hbar\Pi_D D, \tag{3.19}$$

$$\dot{\Pi}_G=\frac{\hbar}{8G^2}-2\hbar\Pi_G^2-\frac{1}{2}m^2-\frac{1}{2}e^2\hbar(A^2+\hbar D), \tag{3.20}$$

$$\dot{\Pi}_D=\frac{\hbar}{8D^2}-2\hbar\Pi_D^2-\frac{1}{2}e^2\hbar^2 G. \tag{3.21}$$

In the leading order large-N approximation, $D=0$, and there is no equation for Π_D.

For numerical work it is sometimes convenient to switch to a set of coordinates where the kinetic terms have the usual canonical form. Defining $\rho_G^2=G$ and $\rho_D^2=D$, the new Hamiltonian is

$$H_H^{(0)}=\frac{1}{2}p_A^2+\frac{1}{2}p_G^2+\frac{1}{2}p_D^2+\frac{\hbar}{8}\left(\frac{1}{\rho_G^2}+\frac{1}{\rho_D^2}\right)+\frac{\hbar}{2}[m^2+e^2(A^2+\hbar\rho_D^2)]\rho_G^2, \tag{3.22}$$

with the resulting equations of motion

$$\dot{A}=p_A, \quad \dot{p}_A=-e^2\hbar A\rho_G^2, \tag{3.23}$$

$$\dot{\rho}_G=p_G, \quad \dot{\rho}_D=p_D, \tag{3.24}$$

$$\dot{p}_G=\frac{\hbar}{4\rho_G^3}-[m^2+e^2\hbar(A^2+\hbar\rho_D^2)], \tag{3.25}$$

$$\dot{p}_D=\frac{\hbar}{4\rho_D^3}-e^2\hbar^2\rho_D\rho_G^2. \tag{3.26}$$

Again the equations for leading order large N are obtained by setting $\rho_D=0$ and dropping p_D. The advantage of this form is the ease in writing symplectic integrators and also simplifying the form of the matrices needed to compute the Lyapunov exponents.

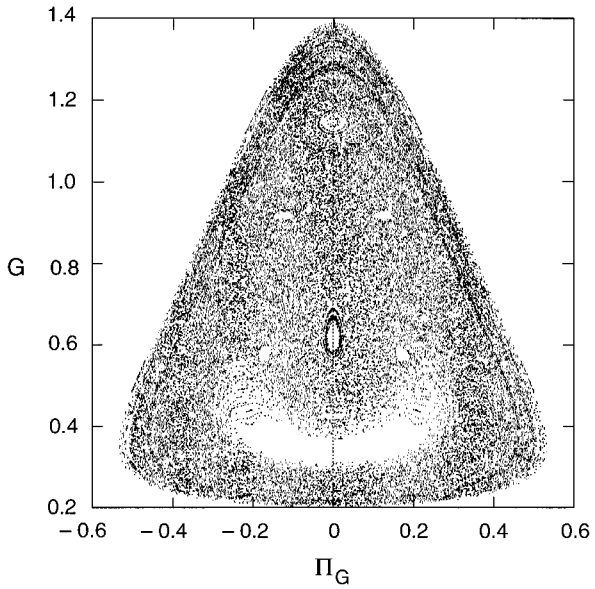

FIG. 4. A Poincaré section in the G, Π_G plane in the large-N approximation for the same set of parameters as Fig. 3.

The above equations can now be solved numerically. Chaos (in the sense of nonzero Lyapunov exponents) exists for large enough values of e^2 and for energy sufficiently above the ground-state energy.

IV. SEMIQUANTUM (GAUSSIAN) CHAOS

A. Numerical methods

In this section we display evidence that both the large-N and Hartree approximations are chaotic for appropriate values of the energy E and the coupling e. (In Ref. [1], the large-N approximation alone was shown to be chaotic.) The dynamics of test trajectories in the above approximations was studied using a fourth order symplectic integrator. (This integrator was implemented using the second set of variables defined at the end of the last section.) Chaos was characterized quantitatively by measuring the Lyapunov exponent for different initial conditions using standard techniques [17].

In order to check whether the chaos seen in the approximation is of some relevance to the full quantum problem, a numerical solution of the corresponding time-dependent Schrödinger equation is required. This was accomplished by using second and fourth order unitary, split-operator, spectral solvers that we have recently implemented on a large parallel computer [18]. By using large grids (up to 4096×4096) sufficient resolution is achieved to accurately evolve the wave function over times long enough to meaningfully compare with results from the variational approximations.

The phase space of the large-N and Hartree approximations was characterized using Poincaré sections. At relatively low energies and modest values of the coupling constant e, both the approximations led to integrable dynamics. However, increasing either the energy or the coupling constant quickly led to nonintegrability. While not carrying out an exhaustive analysis, we did isolate parametric regions where the chaos was relatively soft (the area of stochastic orbits was small compared to the area occupied by regular orbits) and regions where the dynamics was predominantly chaotic.

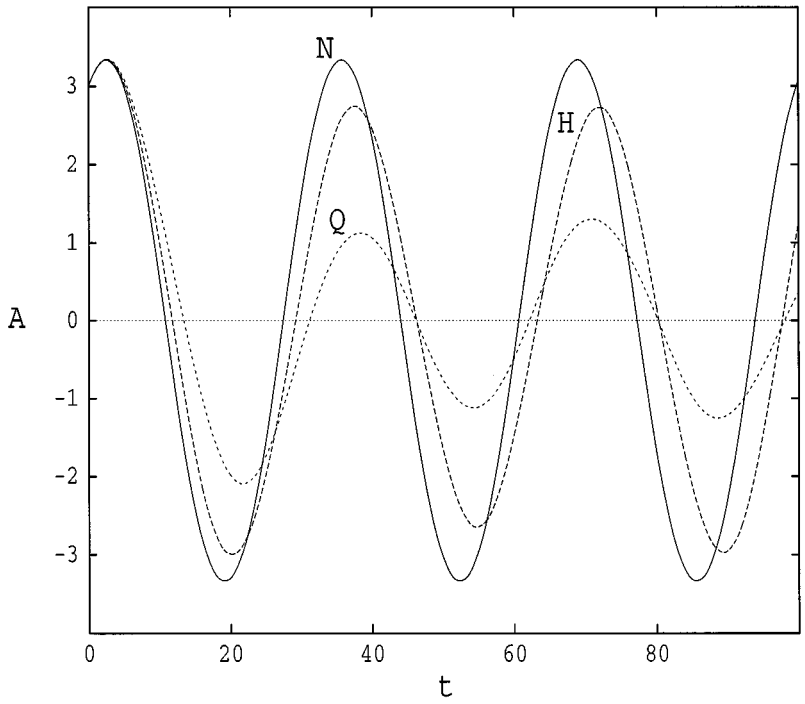

FIG. 5. Evolution of $\langle A \rangle$ for $e=0.3$ and $E=1$. This is within the parameter range for nonchaotic evolution within the approximations. Both approximations break away from the exact evolution at $t \sim 5$ but stay in phase at later times. The Hartree approximation (H) does better in tracking both phase and amplitude. The curve with the smallest average amplitude corresponds to the exact quantum evolution (Q), and the one with the largest average amplitude corresponds to the large-N expansion (N).

We also ran a large set of initial conditions to sample the regions in coupling constant–energy space where the approximations were regular. This was accomplished by implementing a parallel code to compute the Lyapunov exponents for a large set of independent trajectories.

B. Numerical results

There are two separate but related questions concerning the variational approximations. The first question relates to how well they track the exact numerical calculations. We find that the approximations break away from the exact calculation on a short time scale independent of whether they are chaotic or not. However, qualitative agreement with the numerical results is much better in the nonchaotic case. The second question refers to the stability of the approximate solutions as well as the exact solution. In the chaotic regime of the approximations, the approximate evolution is sensitively dependent on initial conditions whereas the exact evolution is not. After a finite time, two approximate evolutions starting from almost identical initial conditions become completely different in the chaotic case and no longer bear any phase relationship among themselves or to the exact solution. This is in contrast with the behavior in the integrable case.

The addition of variational parameters has two effects: it qualitatively improves the long time behavior in both the regular and chaotic regimes even though the break time from the exact behavior is not affected. Secondly, there is some evidence that the onset of chaos is delayed as more parameters are added and that the value of the maximum Lyapunov exponent is also decreased. However, an exhaustive study would require a systematic method of adding variational parameters for the trial wave functions and this we leave to the future.

In Fig. 1 the approximate region of regularity for the large-N approximation is displayed. Each (e,E) point was sampled by ten trajectories, with the Lyapunov exponent cal-

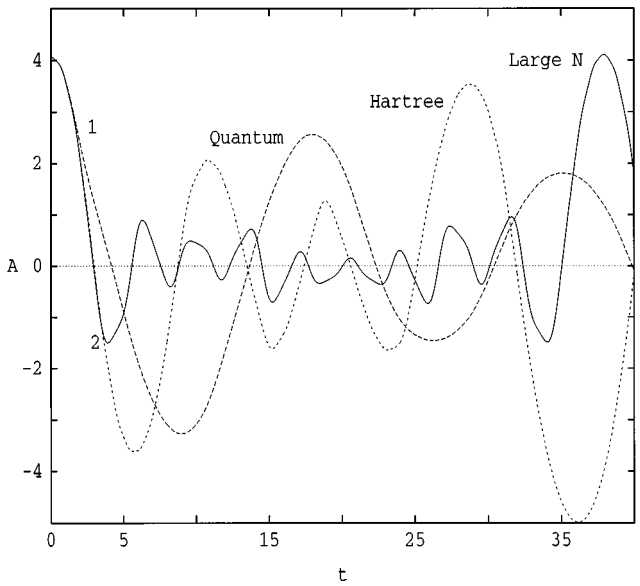

FIG. 6. Evolution of $\langle A \rangle$ for $e=1$ and $E=5$. The approximate evolutions are now chaotic. They break away from the quantum evolution at time $t \sim 2$ (denoted by the point 1 in the figure) and break away from each other at point 2 ($t \sim 4$). In this case the evolutions quickly dephase from each other and from the quantum evolution.

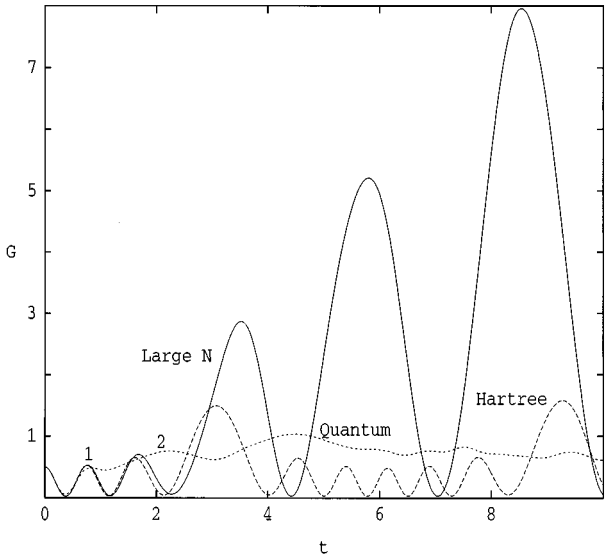

FIG. 7. Evolution of G for the same parameters as Fig. 6. The break from the quantum evolution occurs at $t\sim 1$ (denoted by the point 1 in the figure) and the approximations break away from each other at point 2 ($t\sim 2$). The quantum evolution is much smoother than the approximations: Though the Hartree approximation is not quantitatively correct, it does not have the big excursions shown by the large-N approximation.

culated for each. Within the uncertainties of our sampling scheme the integrable and nonintegrable regions cannot be sharply distinguished: the top set of points denotes at least one trajectory having an asymptotically positive Lyapunov exponent while below the bottom set of points no such trajectory was ever found. The true boundary should be roughly in the middle of these two curves. The results for the Hartree approximation are very similar and slightly above the integrability curve for large N but the difference is of order the uncertainty band. Whether there is a general (monotonic) tendency for this to happen as the number of degrees of freedom is further increased is an interesting speculation which needs to be explored further.

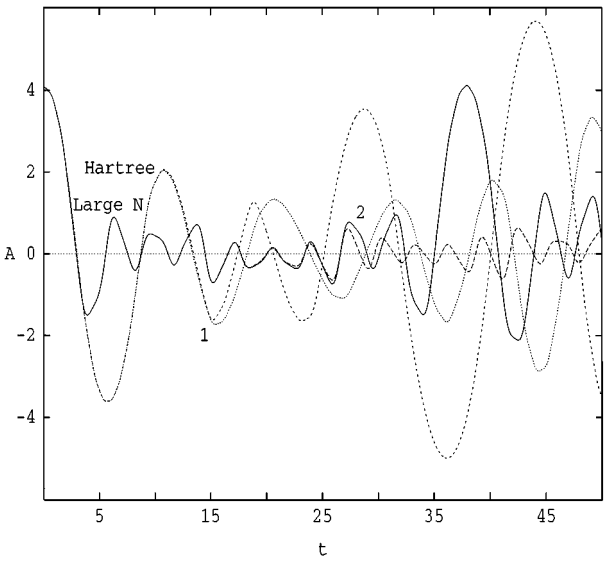

FIG. 8. Evolution of $\langle A\rangle$ for the same parameters as Fig. 6. Points 1 and 2 mark the breaking away of two nearby trajectories in the Hartree and large-N approximations (one of which is the solid line). After this time, the trajectories rapidly dephase from each other.

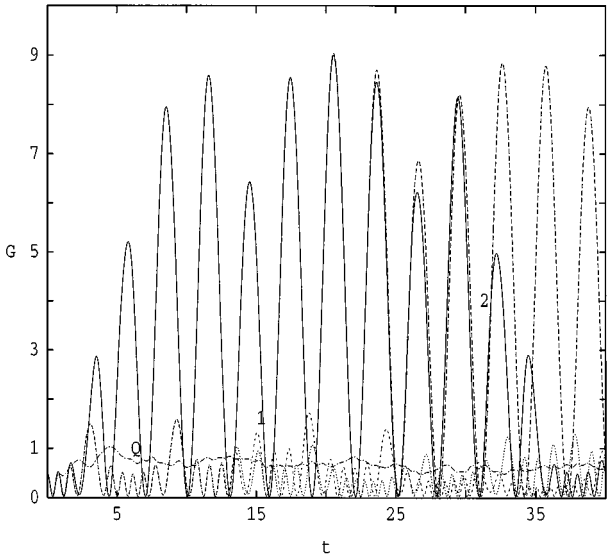

FIG. 9. Evolution of G for the same parameters as Fig. 6. The trajectory denoted by Q is the quantum evolution (recognized also by being the smoothest). Points 1 and 2 mark the breaking away of two nearby trajectories in the Hartree and large-N approximations.

The Lyapunov exponents for the two approximations were computed in the chaotic parameter regime. For all cases we studied the maximal exponent in the Hartree approximation was less than the corresponding exponent in the large-N approximation. A typical example of these results is given in Fig. 2.

Poincaré sections are another way to explore the domains of integrability for the two approximations. For the ''bound-

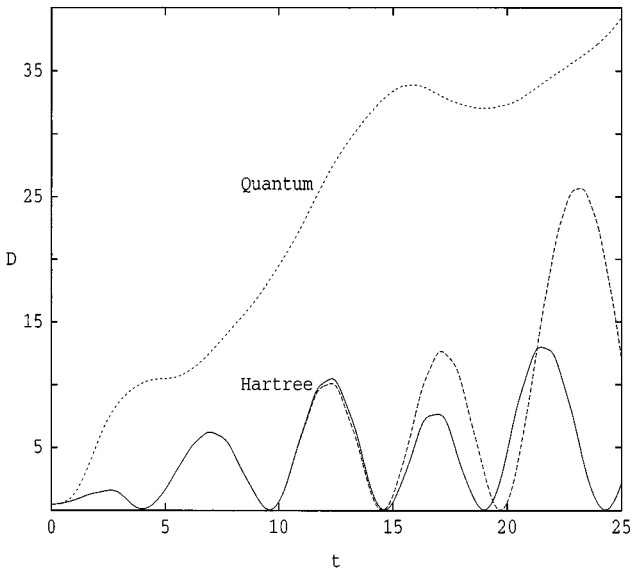

FIG. 10. Evolution of D for the same parameters as Fig. 6. The quantum evolution and the Hartree approximation deviate from each other at $t\sim 1$ and the two nearby trajectories of the Hartree approximation break from each other at $t\sim 15$.

ary'' regions of Fig. 1, the phase space was largely mixed, with stochastic regions coexisting with regular regions. We checked for random values of the parameters that the region below this boundary was regular. Above, it was dominantly chaotic. It was difficult to use Poincaré sections for the Hartree approximation because more degrees of freedom means running much longer to get acceptable statistics. We did run checks for a few parameter values and found results consistent with Fig. 1 including the fact that chaos occurred at larger values of the parameters. For example, while the large-N approximation had appreciably chaotic regions at $E=0.8$, $e=0.7$ the Hartree approximation was completely integrable for those values of the parameters. (Note that the energy E is different for the large N and Hartree approximations since D and Π_D contribute in the Hartree approximation, but not in large N.) For the parameter values, $e=1$ and $E=0.8$ we show two Poincaré sections in Figs. 3 and 4 (large N), which are typical for values of the parameters near the boundaries of Fig. 1.

In order to assess the relevance of the chaos seen in the approximations we have compared the approximate evolutions with exact numerical solutions of the Schrödinger equation with Gaussian initial data. The exact evolution shows no hint of the sensitivity to initial conditions exhibited by the approximate dynamics. As illustrated in Figs. 5, 6, and 7, in both the regular and chaotic regimes the approximations quickly deviate from the exact results on a time scale of order unity, this signaling the breakdown of the Gaussian approximation.

The Lyapunov time sets a maximum time for which the approximations can agree with the exact quantum dynamics. In fact, consistent with this statement we observe that the time of breakdown of the approximations and the Lyapunov time are of the same order. However, this should not lead one to conclude that the accuracy dramatically improves when the approximate dynamics is integrable. Indeed, even in integrable parameter regimes, the breakdown time can remain of order unity (Fig. 5). Therefore, for coupling constants of order unity, these approximations tend to be rather poor. This is because significant non-Gaussian structure forms in the exact wave functions relatively rapidly.

The chaos inherent in the approximations is demonstrated in Figs. 8, 9, and 10, for the evolution of $\langle A\rangle$, G, and D. In these figures we show two trajectories for each of the approximations, one corresponding to an initial $G=0.5$ and the other to $G=0.5001$ (all other parameters held fixed). The deviations of these two curves are consistent with the calculated Lyapunov exponent (which is of order unity) and an initial deviation of order 10^{-4}.

The approximations discussed here break down whenever there is significant non-Gaussian structure in the actual wave function. As long as the coupling is of order unity this happens relatively rapidly. Examples of the numerically evaluated probability densities in A are shown in Figs. 11 and 12 for values of the parameters that correspond to integrable and nonintegrable evolutions.

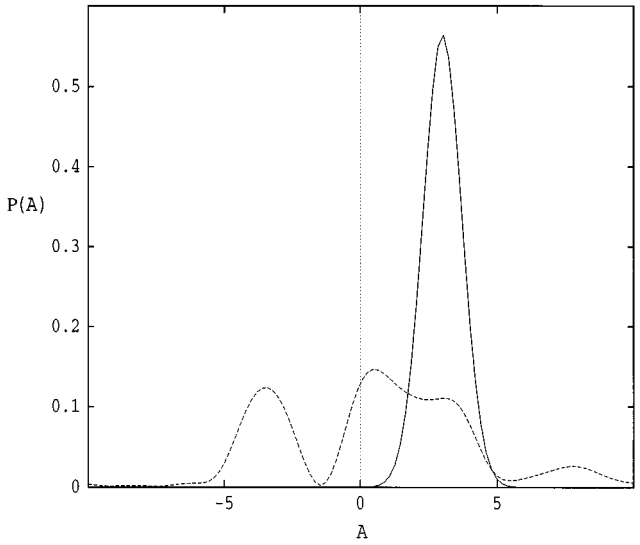

FIG. 11. The initial and final ($t=100$) probability densities for A with $e=0.3$ and $E=5$ (integrable case).

V. CONCLUSIONS

The central results of this investigation may be encapsulated succinctly: all time-dependent variational approximations based on a Dirac approach are Hamiltonian and generically nonlinear. Therefore all such approximations can be chaotic. Since exponential divergence of expectation values in time is ruled out in full quantum mechanics, the Lyapunov time associated with the approximate evolution sets a time scale beyond which the approximation breaks down. We have investigated this last point in two particular examples (large N and Hartree for a two-dimensional potential), find both to be chaotic, and by comparison against numerically obtained solutions, show explicitly that the approximations break down on the Lyapunov time scale. We also show that even in nonchaotic regimes, the approximations break down very quickly. Thus the mere absence of chaos is not an indicator of the accuracy of these approximations.

We would also like to point out that suggestions have been made in the literature that semiquantum chaos may in fact be a real effect (e.g., Ref. [3] and rather more strongly in

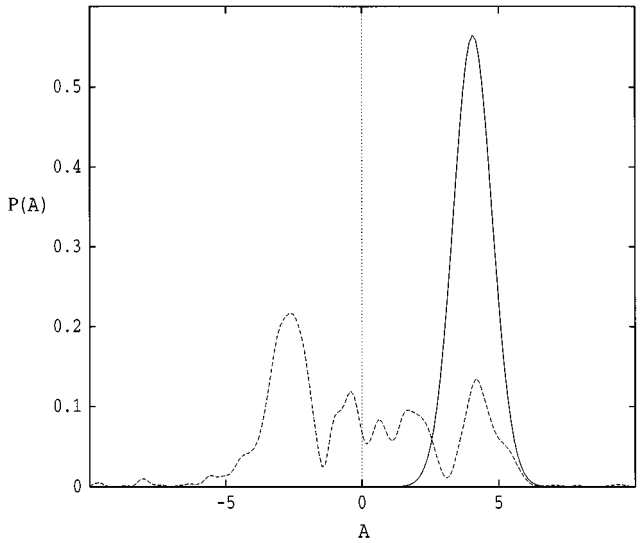

FIG. 12. Same as Fig. 11 with $e=1$, $E=5$ (nonintegrable case). In this case the final time, $t=40$.

Ref. [19]). However, these claims were not backed up by careful comparisons with exact calculations. The detailed results reported here, along with the fact that Gaussian approximations are dynamically completely classical [10], imply exactly the opposite conclusion (in substantial agreement with the arguments of Refs. [4,12]).

The fact that in the chaotic regime, the approximation signals its own breakdown has an interesting physical consequence: if the $1/N$ approximation is in fact sensible then a breakdown at leading order must imply that the next-to-leading terms are becoming large on the same time scale. Since, in field theory the leading order approximation does not incorporate collisions, what this implies is that the collisional time scale can be estimated from the breakdown of the leading order result itself, without actually having to compute the next-to-leading order contribution. Given the complexity of higher order calculations this feature may be extremely useful. This and other aspects of the field theoretic problem are now under investigation.

One way of incorporating higher order correlation functions in dynamical approximations is to consider trial wave functions of the form Gaussian times polynomials. This can be put in correspondence with the large-N expansion, which can be shown to lead to the same structure as higher-order corrections in $1/N$ are added. An interesting question is whether opening up the possibility of including higher order correlations in this way will improve the long time behavior of the variational approach.

ACKNOWLEDGMENTS

The authors acknowledge helpful conversations with Peter Milonni, Emil Mottola, Arjendu Pattanayak, Bala Sundaram, and George Zaslavsky. The large-scale numerical work was performed on the CM5 at the Advanced Computing Laboratory, Los Alamos National Laboratory.

[1] F. Cooper, J. Dawson, D. Meredith, and H. Shepard, Phys. Rev. Lett. **72**, 1337 (1994).
[2] F. Cooper, J. Dawson, S. Habib, Y. Kluger, D. Meredith, and H. Shepard, Physica D **83**, 74 (1995).
[3] A. Pattanayak and W. C. Schieve, Phys. Rev. Lett. **72**, 2855 (1994).
[4] E. Caurier, S. Drożdż, J. Okolowicz, and M. Ploszajczak, Acta Phys. Pol. B **22**, 389 (1991).
[5] Y. Kluger, J. Eisenberg, B. Svetitsky, F. Cooper, and E. Mottola, Phys. Rev. Lett. **67**, 2427 (1991).
[6] F. Cooper, S. Habib, Y. Kluger, E. Mottola, J. P. Paz, and P. R. Anderson, Phys. Rev. D **50**, 2848 (1994).
[7] J. Schwinger, Phys. Rev. **82**, 664 (1951).
[8] S. Habib, Y. Kluger, E. Mottola, and J. P. Paz, Phys. Rev. Lett. **76**, 4660 (1996).
[9] K.-K. Kan, Phys. Rev. A **24**, 2831 (1981).
[10] S. Habib, F. Cooper, E. Mottola, R. D. Ryne, and K. Shizume (unpublished).
[11] See, e.g., R. L. Ingraham, M. E. Goggin, and P. W. Milonni, in *Coherence and Quantum Optics VI*, edited by J. H. Eberley *et al.* (Plenum Press, New York, 1990).
[12] B. Sundaram and P. W. Milonni, Phys. Rev. E **51**, 1971 (1995).
[13] J. Ford, Phys. Rep. **213**, 271 (1992).
[14] P. A. M. Dirac, Proc. Cambridge Philos. Soc. **26**, 376 (1930). See also, F. Cooper, S.-Y. Pi, and P. Stancioff, Phys. Rev. D **34**, 3831 (1986), and references therein.
[15] A. K. Rajagopal and J. T. Marshall, Phys. Rev. A **26**, 2977 (1982).
[16] A. Das, *Integrable Models*, Lecture Notes in Physics Vol. 30 (World Scientific, Singapore, 1989).
[17] A. Wolf, J. B. Swift, H. L. Swinney, and J. A. Vastano, Physica D **16**, 285 (1985).
[18] R. D. Ryne and S. Habib (unpublished); S. Habib and R. D. Ryne (unpublished).
[19] T. Blum and H.-Th. Elze, Phys. Rev. E **53**, 3123 (1996).